Mathematics and Statistics 10(2): 454-462, 2022
DOI: 10.13189/ms.2022.100221 http://www.hrpub.org

Effect of Parameter Estimation on the Performance of Shewhart $\left(\bar{X}, R\right)$-joint Chart Looked at in Terms of the Run Length Distribution

Ugwu Samson O.[1,*], **Nduka Uchenna C.**[1], **Eze Nnaemeka M.**[1], **Odoh Paschal N.**[2], **Ugwu Gibson C.**[3]

[1]Department of Statistics, University of Nigeria Nsukka, Nigeria

[2]Department of Industrial Mathematics and Statistics, Enugu-State of Science and Technology, Nigeria

[3]Department of Statistics, Enugu-State, Institute of Management and Technology, Nigeria

Received October 12, 2021; Revised December 31, 2021; Accepted January 16, 2022

Cite This Paper in the following Citation Styles

***(a)**: [1] Ugwu Samson O., Nduka Uchenna C., Eze Martin N., Odoh Paschal N., Ugwu Gibson C., "Effect of Parameter Estimation on the Performance of Shewhart $\left(\bar{X}, R\right)$-joint Chart Looked at in Terms of the Run Length Distribution," Mathematics and Statistics, Vol.10, No.2, pp. 454-462, 2022. DOI: 10.13189/ms.2022.100221*

***(b)**: Ugwu Samson O., Nduka Uchenna C., Eze Martin N., Odoh Paschal N., Ugwu Gibson C., (2022). Effect of Parameter Estimation on the Performance of Shewhart $\left(\bar{X}, R\right)$-joint Chart Looked at in Terms of the Run Length Distribution. Mathematics and Statistics, 10(2), 454-462 DOI: 10.13189/ms.2022.100221*

Abstract Using spread-charts to monitor process variation and thereafter using the $\bar{x}$-chart to monitor the process mean after is a common practice. To apply these charts independently using estimated 3-sigma limits is common. Recently, some authors considered the application of $\bar{x}$ and R- charts together as a charting scheme, $\left(\bar{X}, R\right)$-chart when the standards are known, Case KK, only the mean standard is known, Case KU and both standards unknown, Case UU. The average run length (ARL) performance criterion was used. However, because of the skewed nature of the run length (RL) distribution, many authors have frowned at the use of ARL as a sole performance measure and encouraged the percentiles of the RL distribution instead. Therefore, the cdfs of the RLs of the chart under the cases mentioned will be derived in this work, and the percentiles are used to look at the chart for Case KU and the yet to be considered case of the chart, Case UK where only the process variance is known is included for comparison. These are the contribution to the existing literature. $\left(\bar{X}, R\right)$-chart performed better in Case KU than in Case UK and the unconditional in-control median run length described the behavior of the chart better than the in-control ARL.

Keywords Average Run Length (ARL), False Alarm Rate (FAR), Median Run Length (MRL), CDF, Joint Chart, Location Chart, Dispersion Chart

1 Introduction

Changes in manufacturing processes are usually tracked and controlled by using control charts. Mainly, these control charts are either used to monitor for location or dispersion parameters of the process distributions. The use of the Shewhart $\bar{x}$-chart to track and control for changes in the process mean (location parameter) is one of the most common applications in statistical process control history and is usually preceded by monitoring for the dispersion parameter as the limits of the Shewhart $\bar{x}$-chart depend on the in-control dispersion parameter of the process distribution. Without this, the results from the Shewhart $\bar{x}$-chart are questionable. The most common control charts for dispersion are the Shewhart R, S, and S^2-charts, see Chen [3]. Therefore, two control charts are used to reach a reliable decision about the state of the process location. The process is considered in control (IC) when the charting statistics of the charts are randomly within the respective limits and out-of-control (OOC) when at

least one chart's statistic is outside the limits or non-random behavior is witnessed, Diko et al. [5]. Reference [5] noted that the common practice in the literature is to apply the Shewhart $\bar{x}$- and R-charts independently, each using the standard or estimated 3-sigma limits and highlighted the scarcity of documented studies considering the design and performance of $\bar{x}$- and R-charts as they are applied together as a charting scheme. The works of Diko [4] considered this scheme for known parameter case (Case KK) while Diko et al. [5] did it for unknown parameter cases, specifically, for Cases (KU $ UU). In line with what has been said, Diko et al. [6] also stated that the common practice when applying these charts is to use the standard 3-sigma limits which are justifiable only when the distribution of the charting statistic is normal or approximately normal. However, the same work added that the distribution of the charting statistics of the R-, S- and S^2-charts are highly skewed, saying that their performance can be quite questionable, particularly for smaller sample sizes. Note that the performance of Phase II quality control charts is often characterized by the run length (RL) distribution and the most popular measure of the performance is the average run length (ARL). However, in the literature, many authors have clearly stated that the run length distribution is generally highly skewed and encouraged the use of more representative measures than the ARL in measuring charts performance, see Chakraborti [2]. Therefore, given this behavior of charting statistic of R-chart and the skewed nature of the RL distribution, it is expected that the run length distributions of the R- and $\left(\bar{X}, R\right)$-charts will be more skewed in distribution. It is well known that the median is a better measure of location in skewed distributions, therefore, the median run length (MRL) and other percentile measures of the RL distribution are better measures of charts performance than the ARL. However, against this background, Diko [4] and Diko et al.[5] who considered $\left(\bar{X}, R\right)$- charting scheme evaluated and reached conclusion on the chart performance in terms of the ARL and the percentage difference between the attained and the nominal in-control ARL values only, which can be highly misleading. Again, recall that Diko et al.[5] highlighted the scanty nature of works in the literature on $\bar{x}$- and R-charts applied together as a charting scheme. Therefore, this work is intended to increase the volume of such works via considering the $\left(\bar{X}, R\right)$-chart scheme when the process mean is unknown but the standard deviation is known (Case UK) which lacks in the literature, however, here, evaluation and charts performance measures are based on the MRL and other representative percentile indices of the RL distribution instead of the ARL. To the best of our knowledge, works on the percentiles of this kind of chart are currently unavailable in the literature and this is a motivation for this study.

The remainder of this paper is structured as follows. The review of the conditional false alarm rate (CFARL) and unconditional in-control average run length (ICARL) for the $\bar{x}$-, R-and the $(\bar{x}, R)$-charting scheme for Case KU are presented in section 2. In section 3, we present the CFAR and the unconditional ICARL for the chart in Case UK. The cdfs and the percentiles of the cdfs are discussed in section 4. Presentation and discussion of results are in section 5 while the conclusion of the work is presented in Section 6.

2 Specified process mean and unspecified process standard deviation (Case KU)

When the process mean standard $\mu = \mu_0$ is given but the process standard deviation σ_0 is not, that is the Case (KU), σ_0 is typically estimated from m historical samples each of size n when the process is in control from the Phase I analysis, Jardim et al.[8]. The estimation is mostly done with any of these three unbiased Phase I estimators; the average range estimator $\left(\bar{R}/d_2(n)\right)$, the average standard deviation estimator $(\bar{s}/c_4(n))$ or the pooled sample standard deviation $s_p/c_4(m(n-1)+1)$, where $d_2(n)$, $c_4(n)$ and $c_4(m(n-1)+1)$ are the unbiasing constants, Goedhart et al. [7]. The choice of the Phase I estimator determines the type of Phase II control chart or combination of charts to be used in the monitoring process. For instance, in Diko et al. [5], the average range estimator was used and that is why the range chart (R-chart) was the choice spread chart for combination with the $\bar{x}$-chart. The choice is the same in this work, therefore, our Phase II control charts will be $\bar{x}$-chart, R- chart and $(\bar{x}, R)$-chart scheme. From henceforth, $d_2(n)$ and $d_3(n)$ will be written as d_2 and d_3 respectively.

2.1 Shewhart $\bar{x}$-chart with 3-sigma limits in Case (KU)

The conditional false alarm rate (CFAR) and unconditional in-control average run length (ICARL) of $\bar{x}$-chart for Case KU with the upper and lower control limits of the chart defined as; $U\hat{C}L = \mu_0 + 3\frac{\hat{\sigma}}{\sqrt{n}}$ and $L\hat{C}L = \mu_0 - 3\frac{\hat{\sigma}}{\sqrt{n}}$ are

$$CFAR_{\bar{x}chart}(y,m,n) = 1 - P\left((\mu_0 - 3\frac{\hat{\sigma}}{\sqrt{n}} < \bar{x_i} < \mu_0 + 3\frac{\hat{\sigma}}{\sqrt{n}})|IC\right) \tag{1}$$

$$= 1 - \Phi\left(3\frac{c\sqrt{y}}{\sqrt{v}}\right) + \Phi\left(-3\frac{c\sqrt{y}}{\sqrt{v}}\right)$$

and

$$ICARL_{\bar{x}chat}(m,n) = \int_0^\infty [CFAR_{\bar{x}chart}(y,m,n)]^{-1} g(y)dy \tag{2}$$

respectively, where it should be noted that; $\sqrt{n}\left(\bar{x}_i - \mu_0\right)/\sigma \sim N(0,1)$, $\hat{\sigma} = \bar{R}/d_2(n)$ is approximately distributed as $\frac{c\sigma\sqrt{y}}{\sqrt{v}}$ and y follows a chi-square distribution with v degrees of freedom, see Diko et al. [5]. The values of c and v depend on m and n and their evaluation is in line with the Patnaik [11] approximation.

2.2 Shewhart R-chart with 3-sigma limits in Case (KU)

The conditional false alarm rate (CFAR) and the unconditional in-control average run length (ICARL) of R-chart with the upper and lower control limits of the chart defined as; $U\hat{C}L = (d_2 + 3d_3)\,\frac{\bar{R}}{d_2}$ and $L\hat{C}L = (d_2 - 3d_3(n))\,\frac{\bar{R}}{d_2}$ are

$$CFAR_{Rchart}\left(y,m,n\right) = 1 - P\left((d_2 - 3d_3)\frac{\bar{R}}{d_2} < R_i < (d_2 + 3d_3)\frac{\bar{R}}{d_2})|IC\right) \tag{3}$$

$$= 1 - P\left(((d_2 - 3d_3)\frac{c\sqrt{y}}{\sqrt{v}} < W_i < (d_2 + 3d_3)\frac{c\sqrt{y}}{\sqrt{v}}))|IC\right)$$

$$= 1 - F_w\left((d_2 + 3d_3)\frac{c\sqrt{y}}{\sqrt{v}}\right) + F_w\left((d_2 - 3d_3)\frac{c\sqrt{y}}{\sqrt{v}}\right)$$

and

$$ICARL_{Rchart}(m,n) = \int_0^\infty [CFAR_{Rchart}\left(y,m,n\right)]^{-1} g(y)dx \tag{4}$$

respectively. Where $W_i = R_i/\sigma$ is the sample relative range, F_w is the cumulative distribution function (cdf) of the relative range and the mean and standard deviation of the in-control distribution of the sample relative range are d_2=E(W) and $d_3 = \sqrt{var(W)}$ respectively.

2.3 Shewhart $(\bar{X},R)$-charting scheme with 3-sigma limits for Case KU

By making use of equations (1), (2), (3) and (4), the CFAR and unconditional ICARL of the $(\bar{X}, R)$-charting scheme are;

$$CFAR_{(\bar{X},R)chart}\left(y,m,n\right) = 1 - [1 - CFAR_{\bar{X}chart}(y,m,n)][1 - CFAR_{Rchart}(y,m,n)] \tag{5}$$

$$= 1 - \left[\Phi\left(3\frac{c\sqrt{y}}{\sqrt{v}}\right) - \Phi\left(-3\frac{c\sqrt{y}}{\sqrt{v}}\right)\right]\left[F_w\left((d_2 + 3d_3)\frac{c\sqrt{y}}{\sqrt{v}}\right) - F_w\left((d_2 - 3d_3)\frac{c\sqrt{y}}{\sqrt{v}}\right)\right]$$

and

$$ICARL_{(\bar{X},R)chart}\left(m,n\right) = \int_0^\infty [CFAR_{(\bar{X},R)chart}\left(y,m,n\right)]^{-1} g(y)dy \tag{6}$$

respectively, see Diko et al. [5]. In this work, the unconditional in-control ARLs of the $\bar{x}$- R- and $(\bar{X}, R)$-charts will be evaluated from equations (2), (4) and (6) respectively for different values of Phase I samples (m) and at n = 5. Throughout this work, n is fixed at this value. The results of the evaluation as carried out in the R statistical package are presented in Table 1 in the ARL column for the respective chart.

3 Unspecified process mean and specified process standard deviation (Case UK)

3.1 Shewhart $\bar{x}$-chart with 3-sigma limits in Case (UK)

Recall that the upper and lower control limits of an $\bar{x}$- control chart under known parameter case are given by; UCL=$\mu_0 + Z_{\alpha/2}\sigma_0/\sqrt{n}$ and LCL=$\mu_0 - Z_{\alpha/2}\sigma_0/\sqrt{n}$ respectively. However, when the mean (μ_0) is unspecified and estimated for but the standard deviation is specified, that is Case UK, the limits become; $U\hat{C}L = \bar{\bar{x}} + Z_{\alpha/2}\sigma_0/\sqrt{n}$ and $L\hat{C}L = \bar{\bar{x}} - Z_{\alpha/2}\sigma_0/\sqrt{n}$ accordingly, where $\bar{\bar{x}} = \sum_{i=1}^{m}\bar{x}_i/m$ is the most common estimator for μ_0, called the grand mean of the m Phase I samples, $Z_{\alpha/2} = \Phi^{-1}(1-\alpha/2)$ is the control limit factor which is 3-sigma limits when $\alpha = 0.0027$, $\Phi(.)$ denotes the standard normal cdf and $\bar{x}_i = \sum_j^n x_{ij}$ is the ith Phase I sample means, see Jardim et al. [8]. The conditional false alarm rate of $\bar{x}$-chart in this case is

$$CFAR_{\bar{x}chart}(Z,m) = 1 - P\left(\bar{\bar{x}} - L\frac{\sigma_0}{\sqrt{n}} \le \bar{x}_i \le \bar{\bar{x}} + L\frac{\sigma_0}{\sqrt{n}}|IC\right) \tag{7}$$

$$= 1 - \Phi\left(Z_{\alpha/2} + \frac{Z}{\sqrt{m}}\right) + \Phi\left(-Z_{\alpha/2} + \frac{Z}{\sqrt{m}}\right)$$

where $Z = \left(\frac{\bar{\bar{x}}-\mu_0}{\sigma_0}\right)/\sqrt{mn} \sim N(0,1)$ and $\Phi(.)$ is as already defined. Therefore, the unconditional ARL is

$$ICARL_{\bar{x}chart}(m) = \int_{-\infty}^{\infty} [CFAR_{\bar{x}chart}(Z,m)]^{-1}\Phi(z)dz \tag{8}$$

$$= 1 - \int_{-\infty}^{\infty} [\Phi\left(Z_{\alpha/2} + \frac{Z}{\sqrt{m}}\right) - \Phi\left(-Z_{\alpha/2} + \frac{Z}{\sqrt{m}}\right)]^{-1}\Phi(z)dz$$

3.2 Three-sigma R-chart under known parameter Case (Case KK)

Under Case UK, the process standard deviation is known and not estimated for in both $\bar{x}$- and R-charts but should be monitored to guarantee correct limits for the $\bar{x}$-chart. Therefore, the R-chart with known parameter limits will be jointly used with $\bar{x}$-chart to monitor for the process location. Given that the process distribution is normal and that the standard deviation (σ_0) of the process is known, the 3-sigma control limits for the R-chart are; $UCL_{Rchart} = E(R)+3\sigma_R$ and $LCL_{Rchart} = E(R)-3\sigma_R$, where $E(R) = d_2\sigma$, $\sigma_R = d_3\sigma$ and d_2, d_3 are functions of the sample size (n) as already defined, see Montgomery [10]. The LCL_{Rchart} is always set at zero (0) to avoid negative limit as the range, R= Y_{max} - $Y_{mini} \geq 0$.

Therefore, CFAR of the R-chart is defined by

$$CFAR_{Rchart}(n) = 1 - P(LCR_{Rchart} \leq R_i \leq UCL_{Rchart}|IC) \tag{9}$$

$$= 1 - P(\sigma(d_2 - d_3) \leq R_i \leq \sigma(d_2 + d_3))$$

$$= 1 - P\left(d_2 - d_3 \leq \frac{R_i}{\sigma} \leq d_2 + d_3\right)$$

$$= 1 - P(d_2 - d_3 \leq W_i \leq d_2 + d_3)$$

$$= 1 - F_w(d_2 + d_3) + F_w(d_2 - d_3)$$

where W_i and F_w are as already defined.

3.3 Shewhart $(\bar{X},R)$-charting scheme with 3-sigma limits for Case UK

By making use of equations (7), (8), and (9), the CFAR and the unconditional ARL of $(\bar{X}, R)$ charting scheme are

$$CFAR_{(\bar{X},R)chart}(Z,m) = 1 - [1 - CFAR_{\bar{x}chart}(Z,m)][1 - CFAR_{Rchart}(n)] \tag{10}$$

$$= 1 - [\Phi\left(Z_{\alpha/2} + \frac{Z}{\sqrt{m}}\right) - \Phi\left(-Z_{\alpha/2} + \frac{Z}{\sqrt{m}}\right)][F_w(d_2 + d_3) - F_w(d_2 - d_3)]$$

and

$$ICARL_{(\bar{X},R)chart}(m) = \int_{-\infty}^{\infty} [CFAR_{(\bar{X},R)chart}(Z,m)]^{-1}\Phi(z)dz \tag{11}$$

where all the parameters are as already defined. The results of the evaluation of equations (8), (11), and the reciprocal of equation (9) are presented in Table 2 in the column labeled ARL for the respective charts.

4 The Run Length Distributions and Percentiles

4.1 The cdfs of $\bar{X}$-, R- and $(\bar{X}, R)$-charts for Case KU

The exact cumulative distribution functions (cdfs) of the $\bar{x}$-, R- and $(\bar{X}, R)$-charts can be deduced from the conditioning and unconditioning approach of Chakraborti [1,2] as follows;

$$P(N \leq s) = 1 - \int_0^\infty [\Phi\left(3\frac{c\sqrt{y}}{\sqrt{v}}\right) - \Phi\left(-3\frac{c\sqrt{y}}{\sqrt{v}}\right)]^s g(y)dy \tag{12}$$

$$P(N \leq s) = 1 - \int_0^\infty [F_w\left((d_2 + 3d_3)\frac{c\sqrt{y}}{\sqrt{v}}\right) - F_w\left((d_2 - 3d_3)\frac{c\sqrt{y}}{\sqrt{v}}\right)]^s g(y)dy \tag{13}$$

and

$$P(N \leq s) = 1 - \int_0^\infty \left(\left[\Phi\left(3\frac{c\sqrt{y}}{\sqrt{v}}\right) - \Phi\left(-3\frac{c\sqrt{y}}{\sqrt{v}}\right)\right]\left[F_w\left((d_2 + 3d_3)\frac{c\sqrt{y}}{\sqrt{v}}\right) - F_w\left((d_2 - 3d_3)\frac{c\sqrt{y}}{\sqrt{v}}\right)\right]\right)^s g(y)dy \tag{14}$$

respectively, where $s = 1, 2, 3, ...$ and the parameters and symbols in them remain as already defined. According to Chakraborti [2], the run length cdfs in equations (12-14) can be used to study the statistical properties and the various performance characteristics of the control charts. The author defined the percentile of a run length distribution to be the smallest integer s such that the cdf at s is at least equal to p. Therefore, equations (12-13) can be redefined for this purpose as

$$1 - \int_0^\infty [\Phi\left(3\frac{c\sqrt{y}}{\sqrt{v}}\right) - \Phi\left(-3\frac{c\sqrt{y}}{\sqrt{v}}\right)]^s g(y)dy \geq p \tag{15}$$

$$1 - \int_0^\infty [F_w\left((d_2 + 3d_3)\frac{c\sqrt{y}}{\sqrt{v}}\right) - F\left((d_2 - 3d_3)\frac{c\sqrt{y}}{\sqrt{v}}\right)]^s g(y)dy \geq p \tag{16}$$

and

$$1 - \int_0^\infty \left(\left[\Phi\left(3\frac{c\sqrt{y}}{\sqrt{v}}\right) - \Phi\left(-3\frac{c\sqrt{y}}{\sqrt{v}}\right)\right]\left[F_w\left((d_2 + 3d_3)\frac{c\sqrt{y}}{\sqrt{v}}\right) - F_w\left((d_2 - 3d_3)\frac{c\sqrt{y}}{\sqrt{v}}\right)\right]\right)^s g(y)dy \geq p \tag{17}$$

The percentile expressions in equations (15), (16), and (17) will equally be evaluated at different values of m and p and the results presented in Table 1 in the percentile columns for the respective charts with the view to studying the performance behaviors of the charts in this perspective. The results will be discussed and compared where necessary.

4.2 The cdfs of $\bar{X}$-, R- and $(\bar{X}, R)$-charts for Case UK

Following what has been said earlier, the exact run length distributions of $\bar{x}$-, R- and $(\bar{X}, R)$-charts under Case UK are given as

$$P\left(N \leq s\right) = 1 - \int_{-\infty}^\infty [\Phi\left(Z_{\alpha/2} + \frac{Z}{\sqrt{m}}\right) - \Phi\left(-Z_{\alpha/2} + \frac{Z}{\sqrt{m}}\right)]^s \Phi(z)dz \tag{18}$$

$$P\left(N \leq s)\right) = 1 - \left[F_w\left(d_2 + d_3\right) - F_w\left(d_2 - d_3\right)\right]^s \tag{19}$$

and

$$P\left(N \leq s\right) = 1 - \int_{-\infty}^\infty \left([\Phi\left(Z_{\alpha/2} + \frac{Z}{\sqrt{m}}\right) - \Phi\left(-Z_{\alpha/2} + \frac{Z}{\sqrt{m}}\right)][F_w\left(d_2 + d_3\right) - F_w\left(d_2 - d_3\right)]\right)^s \tag{20}$$

while the percentiles are given by

$$1 - \int_{-\infty}^\infty [\Phi\left(Z_{\alpha/2} + \frac{Z}{\sqrt{m}}\right) - \Phi\left(-Z_{\alpha/2} + \frac{Z}{\sqrt{m}}\right)]^s \Phi(z)dz \geq p \tag{21}$$

$$1 - \left[F_w\left(d_2 + d_3\right) - F_w\left(d_2 - d_3\right)\right]^s \geq p \tag{22}$$

and

Table 1. The Unconditional ARL and Percentile values of $\bar{X}$-, R- and ($\bar{X}$,R)-charts for KU at different m

	X-chart	Percentiles					
m	ARL	5	25	50	75	90	95
5	3168.65	8	60	226	891	1990	3707
10	884.43	12	76	236	694	1830	3300
20	550.30	15	89	244	601	1291	2019
30	478.56	16	94	247	571	1135	1682
50	430.43	17	98	250	547	1018	1438
100	398.77	18	102	253	529	933	1268
500	375.81	19	106	256	516	868	1140
1000	373.07	19	106	256	514	860	1124
10000	370.64	19	106	257	513	853	1110
	R-chart						
5	11906.82	3	28	129	682	3555	4002
10	999.75	5	38	135	478	1551	3223
20	422.37	7	47	140	386	941	1604
30	332.11	8	51	143	357	778	1229
50	277.91	9	55	145	334	660	973
100	244.98	10	59	148	316	577	804
500	222.43	11	62	150	304	515	679
1000	217.44	11	62	150	302	507	664
10000	199.99	11	62	150	301	500	651
	$(\bar{X}, R)$-chart						
5	2228.02	2	19	82	383	1698	2011
10	444.51	4	26	86	281	833	1616
20	234.77	5	31	89	233	541	888
30	194.21	6	33	90	218	460	706
50	168.16	6	36	92	206	399	578
100	151.60	7	37	93	198	356	490
500	138.52	7	39	95	191	323	425
1000	137.30	7	39	95	191	319	417
10000	136.77	7	39	95	191	316	410

$$1-\int_{-\infty}^{\infty}\left([\Phi\left(Z_{\alpha/2}+\frac{Z}{\sqrt{m}}\right)-\Phi\left(-Z_{\alpha/2}+\frac{Z}{\sqrt{m}}\right)][F_w\left(d_2+d_3\right)-F_w\left(d_2-d_3\right)]\right)^s \geq p \tag{23}$$

respectively, where all the parameters remain as defined earlier.

The results of the evaluations of equations (21), (22), and (23) for the percentiles of the charts are presented in Table 2 in the percentile columns for the respective charts for possible discussions and comparison.

5 Presentation and Discussion of Results

5.1 Discussion of Results

Many authors in the literature have substantiated the fact that the use of parameter estimates rather than the known parameter values affects the performance of the charts negatively unless adjustments are made for the additional variability caused by the parameter estimation see [9], [12]. Based on this, it is a common experience to obtain the unconditional ICARL that is way off (most often less) than the desired $ICARL_0$ and MRL_0 such as 370 and 257 respectively, obtained under known parameter for α_0=0.0027. However, the parameters in real life are often estimated for and not specified. Too, not all the charting statistics of the charts are normally distributed to support the augment of the use of the 3-sigma control limits which is often used in practice.

From Table 1, it is clear that for small to moderate values of m, the unconditional ICARL and ICMRL for the $\bar{x}$-chart are far different from the desired 370 and 257 respectively and such is undesired of a chart as stated earlier. However, as m becomes large, the difference between the desired ARL from the obtained ICARL one thins off and converges at large values of m, say $m \geq 1000$. The same behavior is seen in MRL.

Table 2. The Unconditional ARL and Percentile values of $\bar{X}$-, R- and ($\bar{X}$,R)-charts for UK at different m

	X-chart	Percentiles					
m	ARL	5	25	50	75	90	95
5	237.63	9	52	141	318	582	795
10	277.84	12	71	179	377	659	880
20	310.93	15	86	209	427	724	954
30	326.108	16	92	222	449	755	990
50	340.85	17	97	235	470	786	1027
100	354.14	18	101	245	490	815	1062
500	366.81	19	106	254	508	844	1098
1000	368.56	19	106	256	510	848	1103
10000	370.18	19	106	257	512	852	1108
(X, R)-chart							
5	107.16	5	28	70	146	253	336
10	118.74	6	33	80	163	275	361
20	126.65	7	36	87	175	292	381
30	129.79	7	37	90	179	299	389
50	132.53	7	38	92	183	305	397
100	134.74	7	39	94	187	310	403
500	136.67	7	39	95	189	314	408
1000	136.911	7	40	95	190	315	409
10000	137.13	7	40	95	190	315	410

The values of the MRL for small to moderate values of m are smaller than the desired 257 which clearly shows the expected increase in the FAR of the chart at such values but keeps approaching this value as m grows large, unlike the ARL which is a lot larger than the desired 370 at small to moderate values of m and approaches it by reduction as m grows. This makes the MRL a more consistent measure of performance than the ARL which is badly affected by the shape of the distribution.

From Table 1 still, but under the R- and $(\bar{X}, R)$-charts, the convergence property of the ARL and MRL with the desired values under the growing value of m was lost even at any large value of m. Contradictory to the well-known behavior of the ARLs of other charts, their unconditional ARLs keep falling further away below the desired value with an increasing value of m. Their ARL and MRL values are far different from what is expected of a 3-sigma limit even at any large value of m. One of the reasons for such is that the plotting statistics of the R-chart has a different sampling distribution other than normal and as such has a different ICARL and ICMRL expected under the normal distribution. The MRL of $(\bar{X}, R)$-chart is a lot different from that of the component charts too. Indeed, very poor performance in terms of excessive false alarms is witnessed with this chart, which underscores what was noted by (Diko et al.[5]) in terms of ARL. The author attributed this to the effect of multiple charting in the scheme. For instance, for m = 5, the ICMRL for $\bar{x}$- and R-charts are 226 and 129 respectively. However, this is 82 in $(\bar{X}, R)$-chart which signifies poor performance in terms of more false alarms by the chart. It should be noted that under an in-control state, the larger the MRL, the more efficient a chart is compared to others operating under the same condition.

From Table 2, $(\bar{X}, R)$-chart for Case UK also under-performed the $\bar{x}$-chart under the same condition which is the same as encountered in Case KU. For instance, for m = 5, the ICMRL for $\bar{x}$-chart is 141 while that of $(\bar{X}, R)$-chart is 70. There is also no convergence of both the ICARL and ICMARL to their nominal values. On comparing the performance of $(\bar{X}, R)$-chart in Cases KU and UK, the ICMRLs values for small to moderate values of m of the chart for Case KU are seen to be larger than those in Case UK. Therefore, the chart performs better in Case KU than in Case UK as estimating the process mean showed a more severe effect in the Case UK with more false alarms which contracted the ICMARL than did the effect of estimating the process variance in Case KU. However, at a large value of m say, $m \geq 500$, the ICMRL of the chart in the two cases converges at 95 and 137.2 for the ICARL. From the unconditional cumulative distribution (cdf) plots of the $(\bar{X}, R)$-chart in the two cases, KU and UK for various values of the in-control Phase I samples (m) in Figures 1 1nd 2 respectively, it can be seen that the UK plot of the chart in Figure 2 raised a more false alarm for all the Phase I samples when compared to the case KU in Figure KU despite that the system is in control. This agrees with what has been said that the chart performs better in the case of KU than it does in the case UK.

6 Conclusion

The $(\bar{X}, R)$-chart under-performed its component charts which grew worse at large values of Phase I samples, m, which is usually of a process control chart behavior. The obtained unconditional ICARL and ICMRL never converged with the nominal

Figure 1. Graph of the cdf curves of the run length of the $(\bar{X}, R)$-chart in case KU for various Phase I samples

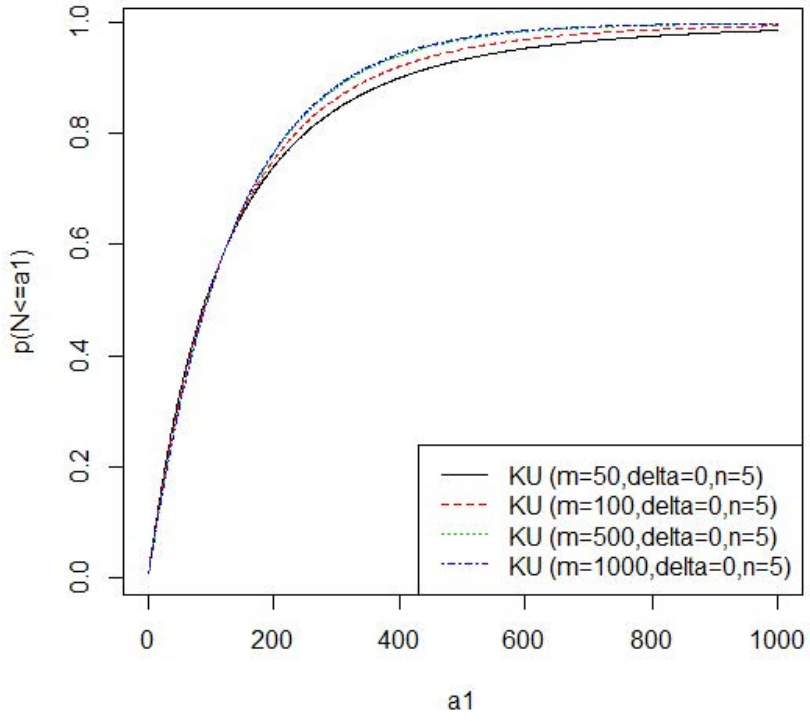

Figure 2. Graph of the cdf curves of the run length of the $(\bar{X}, R)$-chart in case UK for various Phase I samples

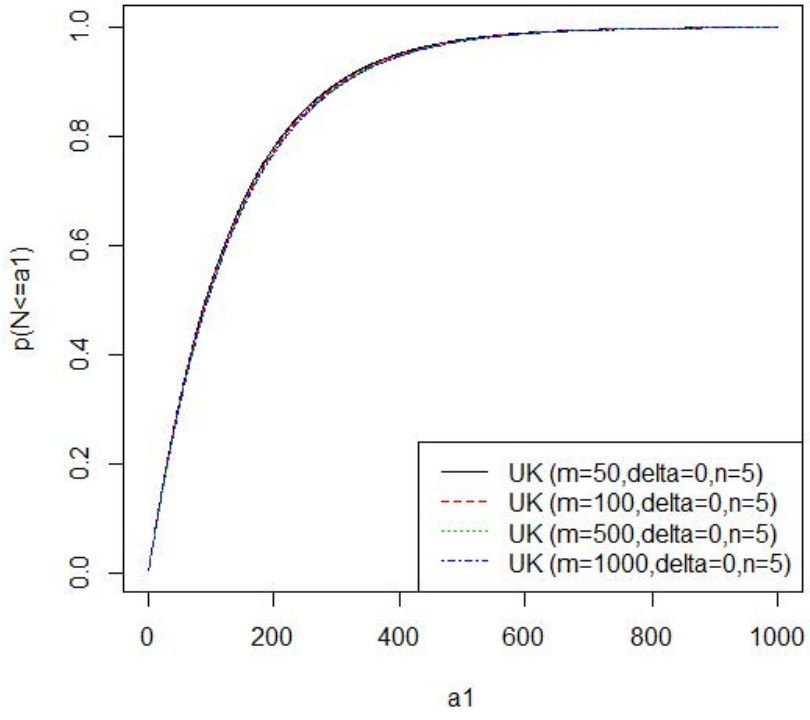

values set for them irrespective of the size of m. When the performance of the chart was compared over the Cases KU and UK, it was discovered to perform better in Case KU. However, at large m, say $m \geq 500$, the performances of the chart in the two cases converge as the ICARL and ICMARL converge and remain at 137.2 and 95 respectively. The unconditional MRL was a more consistent measure of the behavior of the chart than the ICARL as the behavior of ICMARL is consistent in the Cases. For instance, the ICARL in Case KU is high for small values of m and the value drops as m grows, however, in Case UK, the value at small m is low but increases as m grows which highlights the gross effect of the skewed shape of in-control run length distribution on the ARL.

REFERENCES

[1] Chakraborti, S. Run length, average run length, and false alarm rate of Shewhart $\bar{x}$-chart: Exact derivations conditioning. Communications in Statistics, Simulation and, Computation, vol. 29 no.1, pp. 61-81,2000. DOI: 10.1080/03610910008813602

[2] Chakraborti, S. Run length distribution and percentiles: The Shewhart Chart with Unknown Parameters. Quality Engineering, vol.19 no.2, pp. 119-127, 2007. DOI: 10/1080/08982110701276653

[3] Chen, G. The run length distributions of R, S, and S^2control charts when σ is estimated. The Canadian Journal of Statistics, vol. 26 no. 2, pp. 311-322,1997. DOI: 10.2307/3315513

[4] Diko, M.D. (2014). Some contributions to joint monitoring of mean and variance of normal populations. Unpublished MSc Dissertation, Department of Statistics, University of Pretoria: South Africa.

[5] Diko, M.D., Chakraborti, S. and Graham. M.A. Monitoring the process mean when the standards are unknown: A classic problem revisited. Quality Reliability Engineering International, vol. 32 no. 2, pp. 609-622, 2015. DOI: 10.1002/qre.1776

[6] Diko, M.D., Goedhart, R., Chakraborti, S., Does, R.J.M.M. and Epprecht, E.K. Phase II control charts for monitoring dispersion when parameters are estimated, Quality Engineering, vol. 29 no. 4, pp. 605-622, 2017. DOI: 10.1080/08982112.2017.1288915

[7] Goedhart, R., Schoonhoven, M. and Does, R.J.M.M. Guaranteed in-control performance for the Shewhart X and $\bar{X}$control charts, Journal of Quality Technology, vol. 49 no. 2, pp. 155-171, 2017.DOI: 10.1080/00224065.2017.11917986

[8] Jardim, F.S, Chakraborti, S. and Epprecht, E.K. Effects of standard deviation estimation on the $\bar{x}$ control chart and adjustment for a guaranteed in-control performance, pp. 349-360, 2016. Conference paper

[9] Jensen, W.A, Jones-Farmer, L.A., and Woodall, W.H. Effects of parameter estimation on control chart properties: a literature review, Journal of Quality Technology, vol. 38 no. 4, pp.349-364, 2006.DOI: 10.1080/00224065.2006.1198623

[10] Montgomery, D.C. "Appendix IV" in Introduction to Statistical Quality Control, 7th ed, John Wiley & Sons, 2013, pp. 1-754

[11] Patnaik, P. B. The use of mean range as an estimator in statistical tests, Biometrika, vol. 37 no. 1, pp. 78-87, 1950. DOI: 10.1080/biomet/37.1-2.78

[12] Quesenberry, C. P. The effect of sample size on estimated limits for x and $\bar{x}$-control charts, Journal of Quality Technology, vol. 25 no. 4, pp. 237–247, 1993. DOI: 10.1080/00224065.1993.11979470